Revista MVZ Córdoba
ISSN: 0122-0268
ISSN: 1909-0544
revistamvz@gmail.com
Universidad de Córdoba
Colombia

Equilibrium, kinetic and thermodynamic of direct blue 86 dye adsorption on activated carbon obtained from manioc husk

Castellar-Ortega, Grey; Mendoza C, Evert; Angulo M, Edgardo; Paula P, Zilena; Rosso B, María; Jaramillo C, Javier

Equilibrium, kinetic and thermodynamic of direct blue 86 dye adsorption on activated carbon obtained from manioc husk
Revista MVZ Córdoba, vol. 24, no. 2, 2019
Universidad de Córdoba, Colombia
Available in: http://www.redalyc.org/articulo.oa?id=69360025021
DOI: https://doi.org/10.21897/rmvz.1700

Artículos Originales

Equilibrium, kinetic and thermodynamic of direct blue 86 dye adsorption on activated carbon obtained from manioc husk

Equilibrio, cinética y termodinámica de la adsorción del colorante DB-86 sobre carbón activado de la cáscara de yuca

DOI: https://doi.org/10.21897/rmvz.1700
Redalyc: http://www.redalyc.org/articulo.oa?id=69360025021

Grey Castellar-Ortega
Universidad del Atlántico, Colombia
greycastellar@mail.uniatlantico.edu.co
http://orcid.org/0000-0002-8333-0042

Evert Mendoza C
Universidad del Atlántico, Colombia
evertmendoza@mail.uniatlantico.edu.co
http://orcid.org/0000-0002-8333-0042

Edgardo Angulo M
Universidad del Atlántico, Colombia
edgangulo@gmail.com
http://orcid.org/0000-0003-4884-5099

Zilena Paula P
Universidad del Atlántico, Colombia
aneliz_0204@hotmail.com
http://orcid.org/0000-0002-6094-9109

María Rosso B
Universidad del Atlántico, Colombia
k.ami.06@hotmail.com
http://orcid.org/0000-0001-7848-3346

Javier Jaramillo C
Universidad de la Costa, Colombia
javierjaramillocolpas@gmail.com
http://orcid.org/0000-0002-5921-1529

Received: 07 May 2018
Accepted: 05 November 2018
Published: 06 May 2019

Abstract:

Objective. To establish by means of experimenting by batch the capacity of removal, the kinetics and adsorption thermodynamics of activated carbon prepared from manioc husk (*Manihot esculenta*) in the removal of direct blue 86 dye. **Materials and methods.** Firstly, the experimental methodology worked on the preparation of activated carbon by chemical activation of manioc husk with H3PO4 calcined at 530°C. In the characterization the texture properties were determined by means of the blue methylene and iodine indices, the basic and acidic functional groups were quantified by the Boehm method, and the proximate analyses were done following the norms ASTM D2867-70, ASTM D2866 and ASTM D2866-94. During the batch studies, the effect of several parameters over the adsorption capacity was evaluated: pH (2, 4, 8 and 10), temperature (25, 30 and 40°C) and initial concentration of the dye (20, 40, 60, 80 and 100 mg/L). Both physicochemical and adsorption characteristics of the activated carbon from manioc husk (CAY) were compared against those of a commercial brand (CAM). **Results.** The results of characterization showed that both carbons have a chemistry heterogeneous surface, acidic for CAY and basic for CAM. The

maximum capacity obtained was 6.1 mg/g for CAY and 3.7 mg/g for CAM. The thermodynamic calculations showed that the removal was spontaneous. The kinetics for both carbon samples fits a pseudo second-order model. **Conclusions.** The activated carbon obtained from the manioc husk can be considered an efficient adsorbent for the removal of dyes.

Keywords: Activated carbon, adsorption, direct blue 86 dye, pollutant.

Resumen:

Objetivo. Establecer mediante experimentos por lote la capacidad de remoción, la cinética y termodinámica de adsorción del carbón activado preparado a partir de la cáscara de yuca (*Manihot esculenta*) en la remoción del colorante azul directo 86. **Materiales y métodos.** La metodología experimental consistió inicialmente en la preparación del carbón activado por activación química de la cáscara de yuca con H3PO4 y su posterior calcinación a 530°C. En la caracterización se determinaron las propiedades de textura mediante el índice de yodo e índice de azul de metileno, se cuantificaron los grupos funcionales orgánicos ácidos y básicos con el método Boehm, y se realizó el análisis próximo siguiendo las normas ASTM D-2867-70, ASTM D2866 y ASTM D2866-94. En el estudio por lote, el efecto de varios parámetros sobre la capacidad de adsorción fueron evaluados: el pH (2, 4, 8 y 10), la temperatura (25, 30 y 40°C) y la concentración inicial de colorante (20, 40, 60, 80 y 100 mg/L). Tanto las características fisicoquímicas como los ensayos de adsorción del carbón activado preparado a partir de la cáscara de yuca (CAY) fueron comparadas con otro de marca comercial (CAM). **Resultados.** Los resultados de la caracterización indican que ambos carbones tienen una química de superficie heterogénea, de naturaleza ácida para el CAY y básica para el CAM. La máxima capacidad obtenida fue 6.1 mg/g para el CAY y de 3.7 mg/g para el CAM. Los cálculos termodinámicos indican que la remoción es espontánea y para ambos carbones la cinética se ajusta al modelo de pseudo segundo orden. **Conclusiones.** El carbón activado obtenido a partir de la cáscara de yuca puede considerarse un adsorbente eficiente en la remoción de colorantes.

Palabras clave: Adsorción, carbón activado, colorante azul directo 86, contaminantes .

INTRODUCTION

Industries such as textiles, leather, printing, cosmetics, pharmaceuticals, plastics and food use different types of dyes that appear in wastewater discharged by some of these industries (1,2,3). The presence of color in water bodies affects biodiversity because it blocks sunlight diminishing photosynthesis considerably (1,4), also, it is widely known that these compounds contain aromatic amines, benzidines and several other toxic aromatic compounds, which are carcinogenic and mutagenic for humans (3,5,6).

The azo dyes represent the very biggest and versatile group of synthetic dyes. They contain one or more azo bonds (-N=N-) a chromophore group in association with other complex structures that contain functional groups such as $-NH_2$, $-SO_3$, -OH (3,7,8). Also, these dyes can make strong coordination compounds with ions of transition metals, such as Ni (II), Cr (III), Co (II) and Cu (II) among others, making stable azo-metals chelates that cannot be metabolized or degraded (2,9).

There are several methods to eliminate dyes in wastewater. Because of the tests results and its versatility in removing different types of dyes, adsorption is considered one of the best (10,11). Most of the commercial systems employ activated carbon as the adsorbent to remove dyes because of its large surface area and pore volume (12), an excellent capacity of adsorption, fast and easy regeneration (13). Perhaps one of the main disadvantages is the usage of not renewable precursors such as coke and charcoal, relatively highly expensive. This way, researchers have been focused on activated carbon production using non-conventional precursors, renewable materials, plentiful and low cost, such as the biomass coming from farm and industry refuse (14,15,16).

Under this context, activated carbon was prepared by chemical activation with H_3PO_4 using manioc husk as the precursor. Physicochemical characteristics were tested, its capacity of adsorption, thermodynamic and kinetics in removal of direct blue 86 dye and, in addition, it was compared against another commercial brand. The parameters of isothermal models for adsorption and kinetics were adjusted to fit the experimental data.

MATERIALS AND METHODS

Activated carbon preparation. Manioc husk was washed with a lot of water to remove the dust and unwanted material, it was left to dry the sun during 3 days and then for 24 h at 105°C (17) in an oven Esco Isotherm® OFA 32TN-9 forced convection brand. Once the husk was dry, it was ground in a MACSA brand mill 300 525V monitor with 4 kW impulsion, until a particle size between 1 and 4 mm was reached (5x18 granulometry, U. S. Standard Sieve). The ground material was washed with deionized water and dried in an oven for 24 h at 105°C. The chemical activation of this precursor was achieved by adding 1 mL of 85% H_3PO_4 solution (18) per each gram of dried and ground husk, this mixture was kept at 25°C during 24 h. Next it was calcined in a furnace for 30 min at 530°C. Finally, the activated carbon was cooled down and washed with concentrated HCl during 6 h with continuous shaking, for the elimination of phosphates and other impurities. Then washed with deionized water until a pH close to 7 using an Orion Star A221 pH meter, drying for 1 h at 105°C and sifted to select the particles sized from 0.500 to 1.680 mm (12x35 granulometry, U. S. Standard Sieve). The Merck commercial activated carbon was only washed with abundant deionized water and dried in an oven at 105 °C for 24 h.

Characterization of activated carbons. It is vitally important to evaluate certain physical and chemical properties of activated carbon, this way, a better interpretation of the mechanisms involved during the process studied. Thus, a proximate analysis of the different adsorbents was carried out, involving humidity content, ashes and volatile material determinations, following the ASTM standards D-2867-70, D2866 and D2866-94 respectively. Two methods determined the size of pores: according to the iodine index following the standard ASTM D4607-94 and, according to adsorption with methylene blue, applying the Chemviron Carbon Company method, which consists in the addition of an amount of activated carbon to a volume of a standard solution of methylene blue. The maximum capacity (q_{max}) was calculated based on equation 1.

$$q_{max}\left(mg \Big/ g\right) = \frac{(C_o - C_e)V}{M} \qquad \text{[ecu1]}$$

Where C_o and C_e are the initial concentration and the dye equilibrium in mg/L, V is the solution volume in liters and M is the activated carbon mass in grams. The point of zero charge (PZC) was determined by putting 0.5 g of adsorbent in 50 mL deionized water into several sample bottles, later the pH was adjusted between 3 and 12 units with solutions of HCl 0.1 M and NaOH 0.1 M. After 48 h final pH was measured. Finally, the Boehm method was used to quantify the presence of organic groups of functional acids and bases (19,20). This test consisted in adding 1 g of activated carbon at 100 mL of solutions of NaOH 0.1 M, Na_2CO_3 0.1 M, $NaHCO_3$ 0.1 M, and HCl 0.1 M during 24 h, each one separately. Finally, an aliquot was taken and titled with standard solutions of NaOH and HCl according to the case. All of the chemical reagents used were analytical grade Merck® brand.

Batch, thermodynamic and kinetic study. Initially, it was prepared a "stock" solution of 1000 mg/L of direct blue 86 dye, a colorant of the copper phthalocyanine type, molecular formula $C_{32}H_{14}CuN_8Na_2O_6S_2$ (Figure 1), from this solution there were prepared dilutions of 20, 40, 60, 80 and 100 mg/L. For each 50 mL in each of these dilutions, 1 g of activated carbon was added, pH was adjusted to 2 with diluted HCl (value selected from the pH effect study) and placed in a horizontal shaker at 120 rpm during 12 h. Finally, it was filtered, an aliquot was taken and the concentration was determined using a spectrophotometer UV-vis Spectronic Genesys 20 model, at a wavelength of 615 nm, previously determined for each scan. Each one of these experiments was realized three times at different temperatures (25, 30 and 40 °C). The capacity of adsorption and the percentage of removal were calculated according to equations 1 and 2. For kinetic

studies, initial concentration conditions of dye were selected in 100 mg/L and pH 2, differently from the last procedure aliquots were taken between 60 and 720 min.

$$\% R = \frac{(C_o - C_e)}{C_o} \times 100\,\% \qquad \text{[ecu2]}$$

A method very similar to the one mentioned before was applied to evaluate the effect of pH over the capacity of adsorption. This method consisted in making a dilution of 100 mg/L, adjusting the pH with diluted HCl and NaOH to get values of 2, 4, 8 10 ± 0.1, at laboratory temperature (25°C).

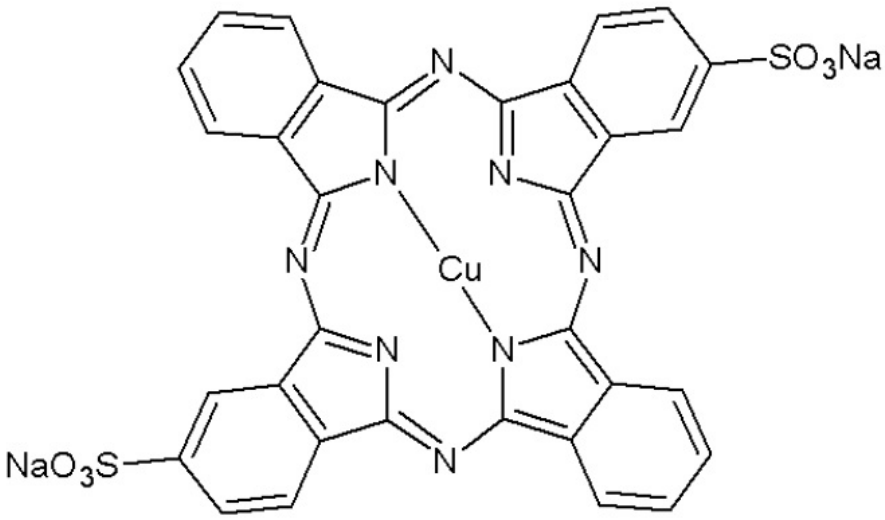

FIGURE 1
Figure 1. Molecular structure of the DB-86 dye.

RESULTS

Physicochemical characterization. The experimental curve of each one of the adsorbents to determine the point of zero charge (PZC) is shown in Figure 2. Values of PZC for activated carbon obtained for the manioc husk and commercial brand carbon are 3.1 and 4.2, respectively. Adsorbents at pH values higher than PZC have a predominant negative charged surface, meanwhile, at a pH lesser than PZC will have a predominant positive charged surface.

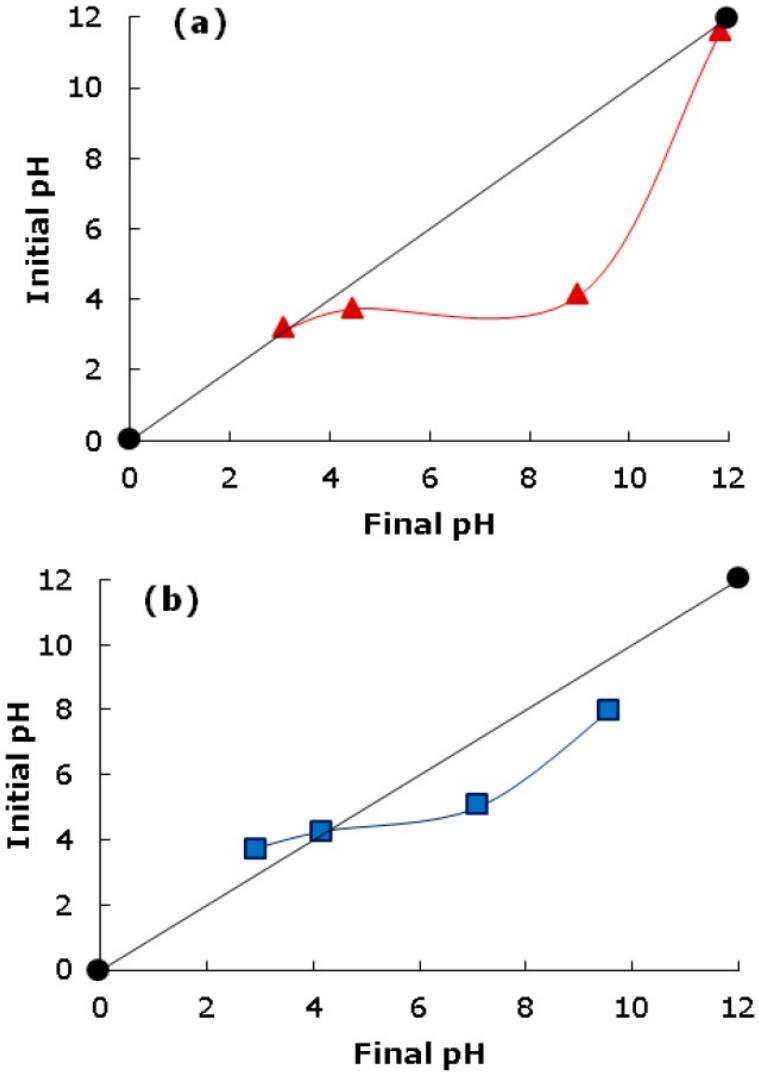

FIGURE 2
Figure 2. Point of zero charge of CAY (a) and CAM (b).

Table 1 shows the physicochemical characteristics of activated carbons CAY and CAM. From the proximate analysis it is observed that the humidity percentage and volatile material it less for the activated carbon prepared from manioc husk than for the commercial carbon brand. On the other side, the content of ashes although low for both activated carbons is slightly higher for CAY. It is suggested that the higher percentage of humidity of the activated carbon CAM (17.4%), is mainly due to its environmental and storage conditions, because as a solid porous adsorbent it retains air humidity on its surface. With respect to the properties of texture: specific area, volume of micropores and total volume of pores, these were calculated from the iodine index and methylene blue index. The iodine index value expresses the amount of iodine adsorption in an aqueous solution, is a measure of micropores and is used as an estimate of the total surface area. Adsorbents with high iodine index show a better performance in the elimination of contaminants of small size, whereas, the methylene blue index shows larger pore sizes developed during activation. It is important to note that for the calculation of the iodine value, samples of 1.2 g of CAY and 1.8 g of CAM were taken, so that the tabulated correction factor of the iodine index would be adjusted to each carbon sample analyzed. In table 1 it is observed that the CAY activated carbon was able to develop a higher specific area (472 m^2/g) with the predominance of micropores that favor the adsorption process. About the bigger

pores size estimation, the methylene blue index shows that the CAM carbon, with 178.5 mg/g, has more macro and mesoporous structures.

TABLE 1

Table 1. Results of the physicochemical characterization of the adsorbents.

Property	Adsorbent	
	CAY	CAM
Proximate analysis		
Moisture (%)	13.1	17.4
Ashes (%)	5.2	3.2
Volatile matter (%)	94.8	96.8
Methylene blue index (mg/g)	62.4	178.5
Iodine index (mg/g)	890	595
Specific area (m^2/g)	472	334
Microporous volume (cm^3/g)	0.23	0.22
Total pore volume (cm^3/g)	0.34	0.54
Acid functional groups		
Phenolic (meq/g)	0.06	0.0
Lactonic (meq/g)	0.0	0.06
Carboxylic (meq/g)	0.62	0.19
Total acidity (meq/g)	0.68	0.25
Total basicity (meq/g)	0.0	0.56

Assuming that NaOH neutralizes carboxylic, lactonic and phenolic groups, Na_2CO_3 neutralizes carboxylic and lactonic groups, $NaHCO_3$ neutralizes only carboxylic groups and HCl neutralizes basic groups, appropriate calculations were made to determine the amount of these functional groups in meq/g for both activated carbons. Results are summarized in table 1.

Batch, thermodynamic and kinetic study. Figure 3 shows how activated carbons adsorption capacity decreases when solution pH increases at 25°C. With lower pH values (2 to 4) the hydronium ion (H^+) concentration increases, charging the activated carbon positively, which helps electrostatic attraction with the DB-86 dye molecules which have an anionic nature. The maximum capacity of adsorption for both activated carbons was reached at pH 2, therefore this pH was chosen.

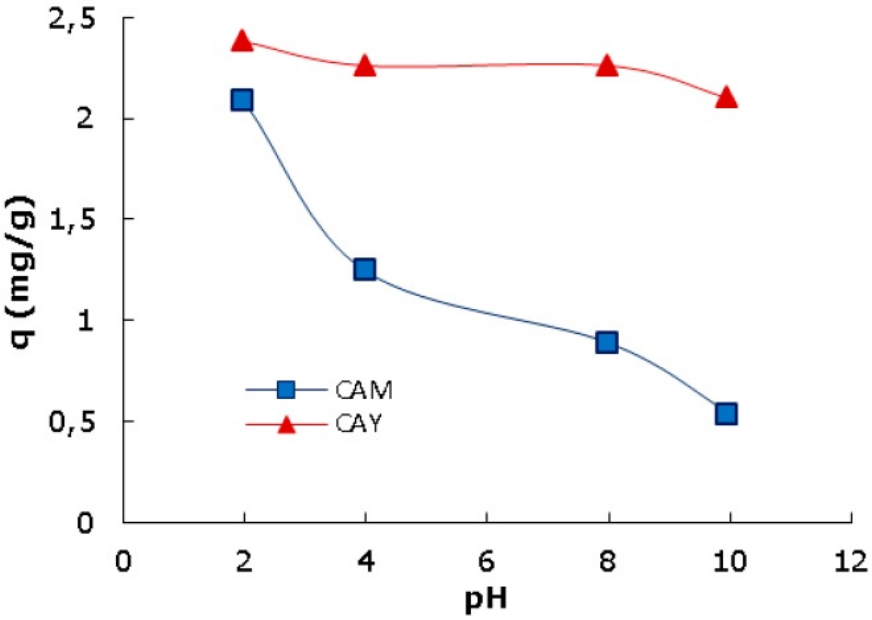

FIGURE 3

Figure 3. Effect of pH on the maximum capacity of adsorption.

Isotherms of adsorption were produced from batch studies, these indicate how adsorbent molecules are distributed between the liquid and solid phases when adsorption reaches its equilibrium state. For this research the data was fitted to Langmuir and Freundlich isotherms models. Linearized equations from both models were represented through equations 3 and 4 respectively.

$$\frac{C_e}{q_e} = \frac{1}{K_L q_{max}} + \frac{C_e}{q_{max}} \quad \text{[ecu3]}$$

$$log q_e = log K_f + \left(\frac{1}{n}\right) log C_e \quad \text{[ecu4]}$$

Where q_{max} (mg/g) is the maximum capacity of adsorption, KL (dm^3/mg) is Langmuir constant and is also related to the heat of adsorption, Kf (mg/g (dm^3/mg)^1/n) is Freundlich constant, n is a constant that indicates the adsorption intensity and C_e (mg/dm^3) is the concentration in the equilibrium. These parameters supply important information about adsorption mechanism, surface properties and adsorbent affinities. Table 2 records these values were adjusted by linear regression.

TABLE 2
Table 2. Parameters of adsorption for isotherms of Langmuir and Freundlich

		Constants of Langmuir			Constants of Freundlich		
Ad	T(°C)	q_{max} (mg/g)	K_L (L/mg)	R^2	n	K_f (mg/g(L/mg)$^{1/n}$)	R^2
CAM	25	3.1	0.015	0.86	0.73	0.007	0.90
CAM	30	3.6	0.032	0.91	1.75	0.246	0.99
CAM	40	3.7	0.036	0.94	1.81	0.277	0.99
CAY	25	6.2	0.008	0.56	1.22	0.080	0.94
CAY	30	3.8	0.029	0.87	1.66	0.223	0.98
CAY	40	3.9	0.033	0.72	1.72	0.260	0.93

Ad= Adsorbent; T=Temperature;

Thermodynamic properties such as Gibbs (ΔG°) energy change, enthalpy (ΔH°) and entropy (ΔS°) were estimated in order to understand the feasibility and nature of the adsorption process (21). From the apparent equilibrium constant stated in equation 3 in the Langmuir isotherm model, Gibbs ΔG° (kJ/mol) change of energy was calculated, for each tested temperatures T (K), using equation 5, where R is the universal constant for gases (8.314 J/molK).

Thermodynamic properties such as Gibbs (ΔG°) energy change, enthalpy (ΔH°) and entropy (ΔS°) were estimated in order to understand the feasibility and nature of the adsorption process (21). From the apparent equilibrium constant stated in equation 3 in the Langmuir isotherm model, Gibbs ΔG° (kJ/mol) change of energy was calculated, for each tested temperatures T (K), using equation 5, where R is the universal constant for gases (8.314 J/molK).

$\Delta G° = -RT \ln K_L$

The Gibbs energy change indicates the grade of spontaneity in the process, negative values reflect a high adsorption and its change can be expressed based on the change in enthalpy ΔH ° (kJ/mol), in entropy ΔS °(J/molK) and the temperature as well, as shown in equation 6.

$\Delta G° = \Delta H° - T\Delta S°$

The following expression can be obtained by replacing equation 5 into 6:

$$InK_L = \frac{\Delta S^{\circ}}{R} - \frac{\Delta H^{\circ}}{RT} \quad \text{[ecu7]}$$

Figure 4 shows the graphic of lnKL vs. 1/T, where the final slope and intersection in the graphic are used to determine ΔH° and ΔS° respectively. Values of thermodynamic properties are summarized in table 3.

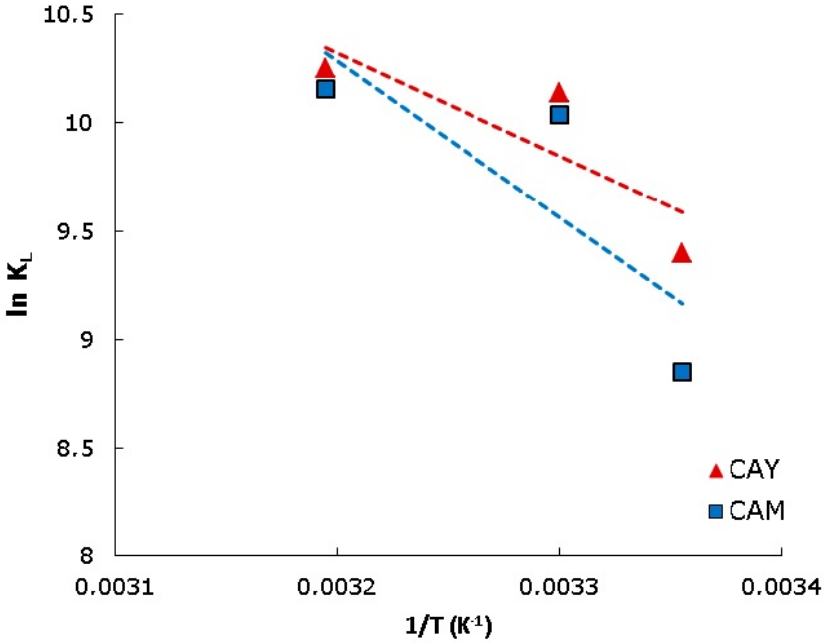

FIGURE 4
Figure 4. Thermodynamics of the adsorption of DB-86 dye on activated carbons CAY and CAM at pH 2.

TABLE 3
Table 3. Thermodynamic parameters of adsorption of the DB-86 dye.

T (°C)	Adsorbent	Thermodynamic parameters K_L (Lmol)	ΔG°(KJ/mol)
25	CAM	12082	-23.3
30	CAM	25399	-25.5
40	CAM	28316	-26.7
25	CAY	6977	-21.9
30	CAY	22877	-25.3
40	CAY	25928	-26.4
Adsorbent	ΔH° (kJ/mol)	ΔS° (J/molK)	R^2
CAM	39.5	212.4	0.70
CAY	60.5	279.1	0.67

With respect to the adsorption kinetics the experimental results were adjusted to the kinetic models of pseudo first-order and pseudo second-order. Equations 8 and 9 show the linearized graphics expressions.

$$log\left(q_e - q_t\right) = log\left(q_e\right) - \left(\frac{k_1}{2,303}\right)t \qquad \text{[ecu8]}$$

$$\left(\frac{t}{q_t}\right) = \frac{1}{k_2 q_e^2} = \frac{t}{q_e} \qquad \text{[ecu9]}$$

Where qe and qt (mg/g) are the capacity of adsorption in equilibrium in a t time respectively and, k_1 (min^{-1}) and K_2(g/mg min) are rate constants for each model (4,22). Values of qe and K_1 were calculated from the linear graphics of $\log(q_e-q_t)$ versus t as shown in figure 5.

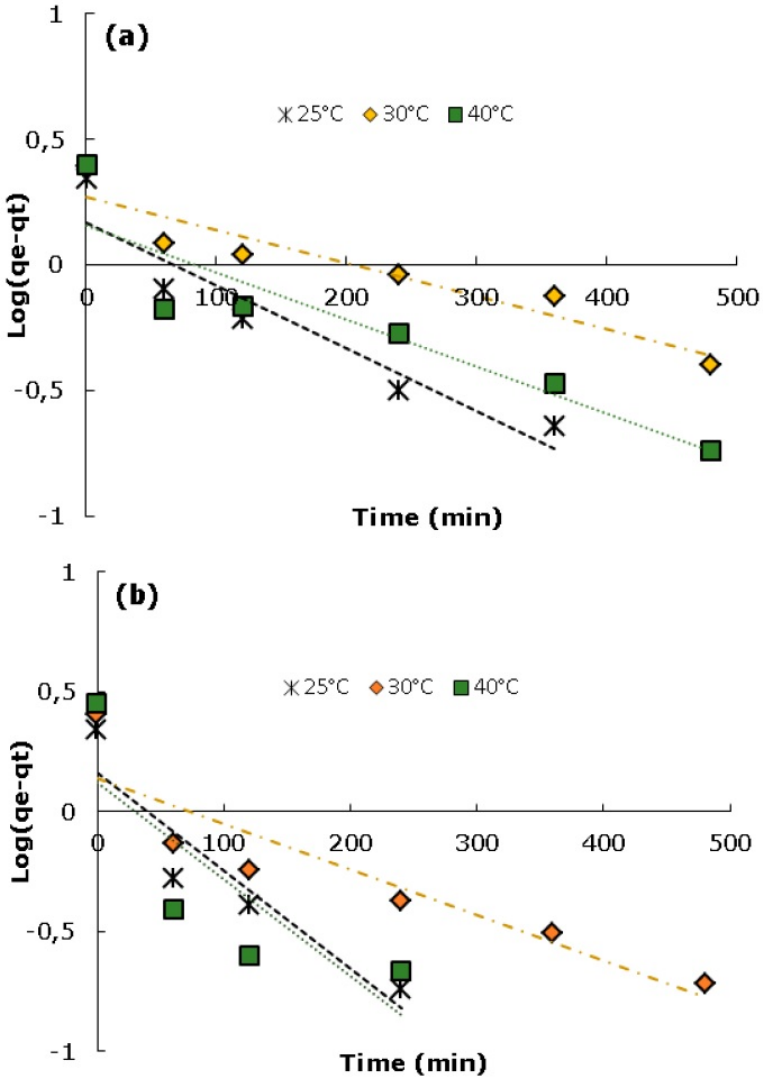

FIGURE 5
Figure 5. Kinetic model pseudo-first order for the adsorption of DB-86 dye at different temperatures: a) CAM and b) CAY.

The same way, values for K_2 and q_e were calculated from the slope and intersection of the straight line from the graphic t/qe versus t (Figure 6). Values for all constants under different temperatures for CAY and CAM carbons can be found in table 4.

TABLE 4

Table 4. Kinetic constants for pseudo-first and pseudo-second order models.

T(° C)	Ad	q_e (exp) (mg/g)	Constants PF			Constants PS		
			k_1 (L/min)	q_e (cal) (mg/g)	R^2	k_2 (g/ (mgmin)	q_e (cal) (mg/g)	R^2
25	CAM	2.2	0.006	1.5	0.89	0.012	2.3	0.99
30	CAM	2.5	0.003	1.9	0.88	0.004	2.6	0.94
40	CAM	2.5	0.004	1.4	0.84	0.009	2.6	0.99
25	CAY	2.2	0.009	1.5	0.87	0.023	2.3	0.99
30	CAY	2.5	0.004	1.4	0.83	0.015	2.5	0.99
40	CAY	2.8	0.009	1.3	0.65	0.037	2.9	0.99

T=Temperature; Ad=Adsorbent; Constants PF: Constants of the kinetic model of pseudo-first order Constants PS: Constants of the kinetic model of pseudo-second order

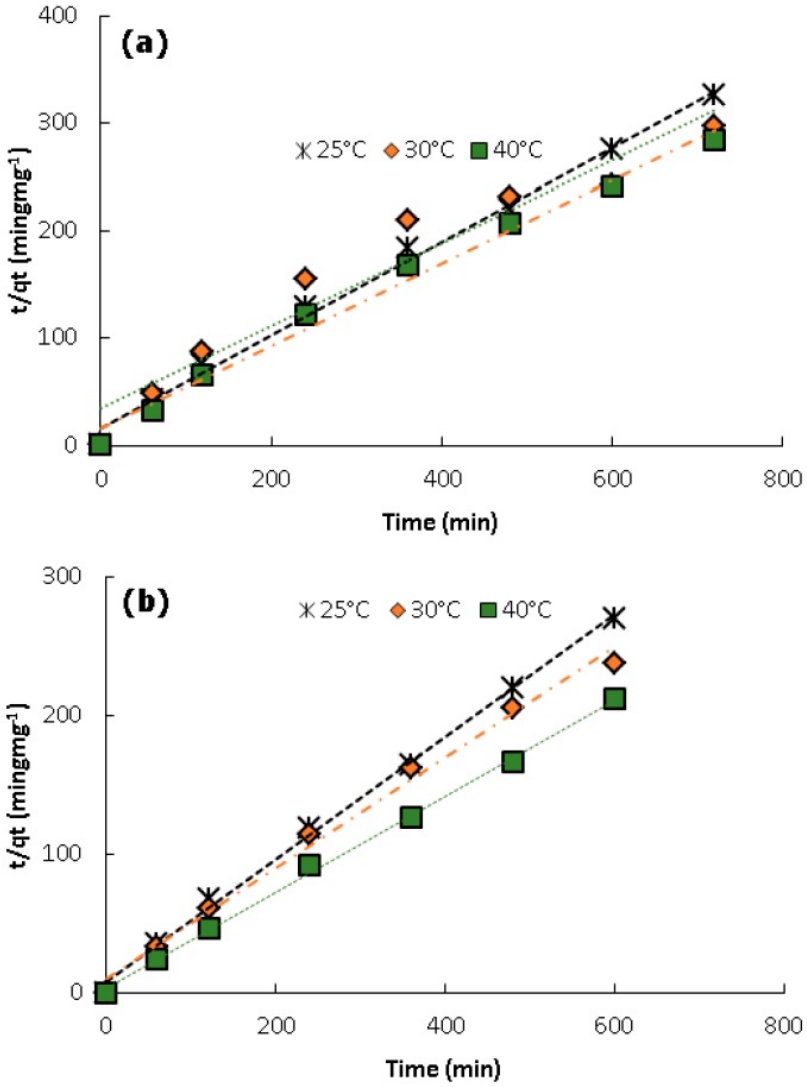

FIGURE 6

Figure 6. Kinetic model pseudo-second order for the adsorption of DB-86 dye at different temperatures: a) CAM and b) CAY.

DISCUSSION

The application of activated carbon as an adsorbent material is associated with surface processes: texture properties and chemical nature. These parameters are intrinsic to the carbon material, that is, they depend on their origin and treatments aimed at modifying their porous structure as well as their surface chemistry. In the case of this investigation the treatment of manioc husk with H_3PO_4 modified both characteristics; with respect to the specific area estimated from the iodine index for both activated carbons, it can be said that it is low in relation to the generic characteristics of this type of adsorbents, as a consequence, surface chemistry plays an important and perhaps relevant role. Factors such as organic functional groups like carboxylic acids (also in the form of their cyclic anhydride), lactones and phenolic hydroxylic groups (Table 1), are responsible for the acid properties of activated carbon (23,24,25) and, the presence of pyrone and chromene structures that imprint electronic density on the graphene layers, especially delocalized π electrons, that are responsible for the basic character.

The activated carbon prepared from manioc husk has a higher content of acid groups (0.68 meq/g), so its pH value in the point of zero charge is 3.1, which is to be expected because it was activated with phosphoric acid. On the other side, though it was not known how the commercial carbon was activated, having a higher meso and macroporosity development (0.32 cm^3/g) makes it decrease its acidity (26).

One of the main factors that affect adsorbing capacity in the wastewater treatment is pH. Figure 3 shows the pH effect on the DB-86 dye removal for the two analyzed carbons. The behavior is very similar: the maximum capacity of adsorption decreases when pH increases. These changes can be attributed to (i) the interactions between the surface functional groups of the adsorbent and the functional groups of the molecules in the dye (sulfonate groups) changing the concentration of H^+ and OH^- and, (ii) the adsorbent interactions with other functional groups (hydrogen bonds and water soluble groups) (10).

In explaining the possible effect of pH, the determination of the zero charge potential (PZC) plays an important role. Taking CAY activated carbon PZC as an example, for pH values over 3.1, negative charges predominate on the carbon surface. For values pH under 3.1, the surface has mainly positive charges.

In the case of the DB-86 dye when mixing it with water it dilutes instantly dissociating its sulfonate groups as follows:

$$D-SO_3NaH_2OD-SO_3^-+Na^+ \quad \text{[ecu10]}$$

At pH 2 whose value is under the PZC, the surface of the activated carbon CAY is charged positively:

$$CAY \xrightarrow{pH<3.1} CAY^+ \quad \text{[ecu11]}$$

As a result, the adsorption process proceeds amply through electrostatic attractions between the two counterions:

$$CAY^+ + D{-}SO_3^- \rightleftharpoons CAY^+{-}O_3S-D \quad \text{[ecu12]}$$

When increasing the solution pH (pH>3.1) the activated carbon surface gets a negative charge:

$$CAY \xrightarrow{pH>3.1} CAY^- \quad \text{[ecu13]}$$

Because the DB-86 dye keeps the negative charges of the sulfonate groups, interactions diminish, so, its adsorption lowers. If the activated carbon CAY keeps removing the dye even at basic pH, it is because of forces like van der Waals and hydrogen bonds.

The parameters of the two adsorption isotherm models were adjusted to the experimental data: (i) The Langmuir model was chosen to estimate the maximum capacity of adsorption, results show that CAY has high capacity with 6.2 mg/g at 25 °C. The coefficient of linear correlation is considerably smaller than 1 for all the temperatures studied (Table 2) , suggesting that the adsorption processes do not happen in identical active sites at the surfaces of the activated carbons, in consequence, the adsorption process is not limited only to covering monolayers and, (ii) the Freundlich model as an empirical equation that can be used for the not-ideal adsorption over a heterogeneous surface; the parameter n is a measure of the deviation of linearity of adsorption. If n equals the unit, adsorption is linear. If n is lower than the unit, then the adsorption process is chemical, but if n is higher than the unit, a physical process is favored according to considerations of this method (27). Table 2 shows that values for n higher than 1, which suggests that physical adsorption is predominant.

Comparing correlation coefficients in both models (Table 2), it is seen that the Freundlich isotherm model best represents the equilibrium of adsorption (R2>0.93) under all evaluated temperatures. This suggests that the adsorption process is wholly carried out over a heterogeneous surface in a multilayer growth.

The negative values of ΔG ° for both activated carbons shows that the DB-86 dye adsorption processes were spontaneous. Similar results that show the spontaneity of the dye adsorption process have been reported by other researchers: Aljeboree et al (4), used coconut husk as a precursor in the preparation of activated carbon and its use in the removal of textile dyes such as direct yellow (DY12) and blue maxilon (GRL); from the rind of the Brazilian pine fruit, Calvete et al (28), prepared activated carbon, which they then used in the removal of the reactive dye orange 16 (RO-16); Leechart et al (29), used the ashes of wood cut waste as a precursor material in the preparation of activated carbon, to later evaluate it in the removal of reactive red dye 141 (RR141); among other investigations.

The positive enthalpy change indicates that the adsorption of DB-86 dye is endothermic. When the attraction between the dye and the adsorbent takes place, the change in the standard enthalpy occurs by the presence of forces that include van der Waals, hydrogen bonds, ligand exchange, dipole-dipole interactions and chemical bonds (30,31). According to the magnitude of the sum of the different forces, the nature of an adsorption can be physical or chemical. Generally, the magnitude of the standard enthalpy change for physical adsorption is close to 20 kJ/mol, while chemisorption is in the range of 80-200 kJ/mol (32). In this study, the calculated enthalpies correspond to 39.5 and 60.5 kJ/mol for the activated carbons CAM and CAY respectively, these values suggest a tendency towards physisorption, because the enthalpy change is below what is required for the occurrence of chemisorption. Concerning the positive change in standard entropy the tendency of the DB-86 dye to adsorb over the surface of the evaluated activated carbons evaluated is confirmed.

About the fitting of experimental data to kinetic models, the equation of pseudo-second order shows an excellent fit with a linear correlation coefficient R^2>0.94 for all temperature conditions. Likewise, the values calculated for q_e from the kinetic model are very similar to those obtained experimentally.

In conclusion, the commercial brand carbon and activated carbon obtained from manioc husk have different chemical composition probably because of different precursors as well as different activation methods. The difference between points of zero charge, texture properties, organic oxygenated functional groups, and other physicochemical properties this is evidenced. The fitting of experimental data to Langmuir and Freundlich isotherms proved that the activated carbon CAY showed the highest adsorption capacity (6.2 mg/g). The best fit was obtained with the pseudo-second order kinetic model and the thermodynamic results demonstrate the spontaneity of the DB-86 dye adsorption over both activated carbons. The development

of a good surface area together with its acidic nature allows the activated carbon obtained from the manioc husk to be used in the removal of DB-86 dye.

Interest conflict

The authors declare no conflicts of interest.

REFERENCES

1. Anirudhan TS, Ramachandran M. Adsorptive removal of basic dyes from aqueous solutions by surfactant modified bentonite clay (organoclay): Kinetic and competitive adsorption isotherm. Process Saf Environ Prot. 2015; 95:215–225. https://doi.org/10.1016/j.psep.2015.03.003
2. Arica MY, Bayramoglu G. Polyaniline coated magnetic carboxymethylcellulose beads for selective removal of uranium ions from aqueous solution. J Radioanal Nucl Chem. 2016; 310(2):711–724. https://doi.org/10.1007/s10967-016-4828-z
3. Bayramoglu G, Akbulut A, Liman G, Arica MY. Removal of metal complexed azo dyes from aqueous solution using tris(2-aminoethyl) amine ligand modified magnetic p(GMA-EGDMA) cationic resin: Adsorption, isotherm and kinetic studies. Chem Eng Res Des. 2017; 124:85–97. https://doi.org/10.1016/j.cherd.2017.06.005
4. Aljeboree AM, Alshirifi AN, Alkaim AF. Kinetics and equilibrium study for the adsorption of textile dyes on coconut shell activated carbón. Arab J Chem. 2017; 10(Supl 2):S3381–S3393. https://doi.org/10.1016/j.arabjc.2014.01.020
5. Castellar G, Angulo E, Zambrano A, Charris D. Equilibrio de adsorción del colorante azul de metileno sobre carbón activado. Rev UDCA Act & Div Cient. 2013; 16(1):263–271. https://revistas.udca.edu.co/index.php/ruadc/article/view/882
6. Chabane L, Cheknane B, Zermane F, Bouras O, Baudu M. Synthesis and characterization of reinforced hybridporous beads: application to the adsorption of malachitegreen in aqueous solution. Chem Eng Res Des. 2017; 120: 291–302. https://doi.org/10.1016/j.cherd.2016.12.014
7. Sari AA, Muryanto ST, Hadibarata T. Development of bioreactor systems for decolorization of Reactive Green 19 using white rot fungus. Desalin Water Treat. 2016; 57(15):7029–7039. https://doi.org/10.1080/19443994.2015.1012121
8. Mirzadeh SS, Khezri SM, Rezaei S, Forootanfar H, Mahvi AH, Faramarzi MA. Decolorization of two synthetic dyes using the purified laccase of Paraconiothyrium variabile immobilized on porous silica beads. J Environ Health Sci Eng. 2014; 12(6):1-9. https://doi.org/10.1186/2052-336x-12-6
9. Tavengwa NT, Cukrowska E, Chimuka L. Synthesis, adsorption and selectivity studies of N-propyl quaternized magnetic poly(4-vinylpyridine) for hexavalent chromium. Talanta. 2013; 116:670–677. https://doi.org/10.1016/j.talanta.2013.07.034
10. Kyzas GZ, Lazaridis NK, Mitropoulos A. Removal of dyes from aqueous solutions with untreated coffee residues as potential low-cost adsorbents: Equilibrium, reuse and thermodynamic approach. Chem Eng J. 2012; 189-190: 148-159. https://doi.org/10.1016/j.cej.2012.02.045
11. Ho YS, McKay G. Sorption of dyes and copper ions onto biosorbents. Process Biochem. 2003; 38(7):1047-1061. https://doi.org/10.1016/s0032-9592(02)00239-x
12. Gonçalves M, Guerreiro M, De Oliveira L, De Castro C. A friendly environmental material: iron oxide dispersed over activated carbon from coffee husk for organic pollutants removal. J Environ Manage. 2013; 127:206-211. https://doi.org/10.1016/j.jenvman.2013.05.017
13. Hu Z, Srinivasan MP. Preparation of high-surface-area activated carbons from coconut shell. Microporous Mesoporous Mater. 1999; 27(1):11-18. https://doi.org/10.1016/s1387-1811(98)00183-8
14. Li G, Zhu W, Zhang C, Zhang S, Liu L, Zhu L, Zhao W. Effect of a magnetic field on the adsorptive removal of methylene blue onto wheat straw biochar. Bioresour Technol. 2016; 206:16-22. https://doi.org/10.1016/j.biortech.2015.12.087

15. Sun L, Chen D, Wan S, Yu Z. Performance, kinetics, and equilibrium of methylene blue adsorption on biochar derived from eucalyptus saw dust modified with citric, tartaric, and acetic acids. Bioresour Technol. 2015; 198:300-308. https://doi.org/10.1016/j.biortech.2015.09.026

16. Jung KW, Choi BH, Hwang MJ, Jeong TU, Ahn KH. Fabrication of granular activated carbons derived from spent coffee grounds by entrapment in calcium alginate beads for adsorption of acid orange 7 and methylene blue. Bioresour Technol. 2016; 219:185-195. https://doi.org/10.1016/j.biortech.2016.07.098

17. Albis A, López AJ, Romero MC. Remoción de azul de metileno de soluciones acuosas utilizando cáscara de yuca (Manihot esculenta) modificada con ácido fosfórico. Prospectiva. 2017; 15(2):60-73. https://doi.org/10.15665/rp.v15i2.777

18. Gonçalves R, Martins C, Mendes N, Farias L, Ferreira RC, Oliveira A, Oliveira M, Ilhéu R. Preparation of activated carbons from cocoa shells and siriguela seeds using H3PO4 and ZnCL2 as activating agents for BSA and α-lactalbumin adsorption. Fuel Process Technol. 2014; 126:476–486. https://doi.org/10.1016/j.fuproc.2014.06.001

19. Boehm HP. Chemical identification of surface groups. Adv Catal. 1966; 16: 179–274. https://doi.org/10.1016/S0360-0564(08)60354-5

20. Nunell GV, Fernández ME, Bonelli PR, Cukierman AL. Conversion of biomass from an invasive species into activated carbons for removal of nitrate from wastewater. Biomass Bioenerg. 2012; 44:87-95. https://doi.org/10.1016/j.biombioe.2012.05.001

21. Figueroa D, Moreno A, Hormaza A. Equilibrio, termodinámica y modelos cinéticos en la adsorción de Rojo 40 sobre tuza de maíz. Rev Ing Univ Medellín. 2015; 14(26):105-120. https://doi.org/10.22395/rium.v14n26a7

22. Konicki W, Aleksandrzak M, Mijowska E. Equilibrium, kinetic and thermodynamic studies on adsorption of cationic dyes from aqueous solutions using graphene oxide. Chem Eng Res Des. 2017; 123:35–49. https://doi.org/10.1016/j.cherd.2017.03.036

23. Contescu A, Contescu C, Putyera K, Schwarz J. Surface acidity of carbons characterized by their continuous pK distribution and Böehm titration. Carbon 1997; 35(1):83-94. https://doi.org/10.1016/s0008-6223(96)00125-x

24. Valencia J, Castellar G. Predicción de las curvas de ruptura para la remoción de plomo (II) en disolución acuosa sobre carbón activado en una columna empacada. Rev Fac Ing Univ Antioquia. 2013; 66:141-158. http://aprendeenlinea.udea.edu.co/revistas/index.php/ingenieria/article/view/15231

25. Maldonado-Hódar FJ, Morales-Torres S, Perez-Cardenas AF, Carrasco-Marín F. Química superficial de los materiales de carbón. Bol Grupo Español Carbón. 2011; 20:10-15. http://www.gecarbon.org/Boletines/articulos/boletinGEC_020_art.3.pdf

26. Rincón-Silva N, Ramirez-Gomez W, Mojica-Sánchez L, Blanco-Martínez D, Giraldo L, Moreno-Piraján J. Obtención de carbones activados a partir de semillas de eucalipto, por activación química con H3PO4. Caracterización y evaluación de la capacidad de absorción de fenol desde solución acuosa. Ingeniería y Competitividad. 2014; 16(1):207-219. https://doi.org/10.25100/iyc.v16i1.3725

27. Kumar PS, Ramalingam S, Senthamarai C, Niranjanaa M, Vijayalakshmi P, Sivanesan S. Adsorption of dye from aqueous solution by cashew nut shell: studies on equilibrium isotherm, kinetics and thermodynamics of interactions. Desalination. 2010; 261(1-2):52–60. https://doi.org/10.1016/j.desal.2010.05.032

28. Calvete T, Lima EC, Cardoso NF, Vaghetti JCP, Dias SLP, Pavan FA. Application of carbon adsorbents prepared from Brazilian-pine fruit shell for the removal of reactive orange 16 from aqueous solution: Kinetic, equilibrium, and thermodynamic studies. J Environ Manage. 2010; 91(8):1695-1706. https://doi.org/10.1016/j.jenvman.2010.03.013

29. Leechart P, Nakbanpote W, Thiravetyan P. Application of 'waste' wood-shaving bottom ash for adsorption of azo reactive dye. J Environ Manage. 2009; 90(2):912-920. https://doi.org/10.1016/j.jenvman.2008.02.005

30. Li Q, Yue QY, Su Y, Gao BY, Sun HJ. Equilibrium, thermodynamics and process design to minimize adsorbent amount for the adsorption of acid dyes onto cationic polymer-loaded bentonite. Chem Eng J. 2010; 158(3):489–497. https://doi.org/10.1016/j.cej.2010.01.033

31. Von Oepen B, Kördel W, Klein W. Sorption of nonpolar and polar compounds to soils: processes, measurements and experience with the applicability of the modified OECD-Guideline 106. Chemosphere. 1991; 22(3-4):285–304. https://doi.org/10.1016/0045-6535(91)90318-8

32. Gu B, Schmitt J, Chen Z, Liang L, McCarthy JF. Adsorption and desorption of natural organic matter on iron oxide: mechanisms and models. Environ Sci Technol. 1994; 28(1):38-46. https://doi.org/10.1021/es00050a007

Additional information

How to Cite: Castellar-Ortega, G., Mendoza Colina, E., Angulo Mercado, E., Paula Pereira, Z., Rosso Bravo, M., & Jaramillo Colpas, J. (2019). Equilibrium, kinetic and thermodynamic of direct blue 86 dye adsorption on activated carbon obtained from manioc husk DB-86 dye adsorption. Journal MVZ Cordoba, 24(2), 7231-7238. https://doi.org/10.21897/rmvz.1700